

# Template-Free Synthesis of Cube-like Ag/AgCl Nanostructures via a Direct-Precipitation Protocol: Highly Efficient Sunlight-Driven Plasmonic Photocatalysts

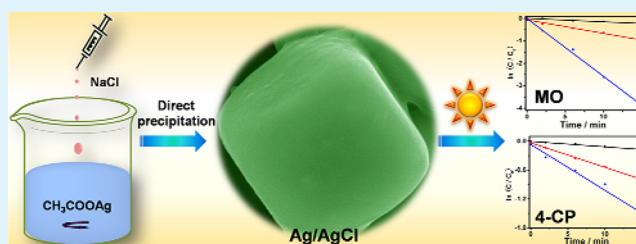
Mingshan Zhu, Penglei Chen,\* Wanhong Ma, Bin Lei, and Minghua Liu\*

Beijing National Laboratory for Molecular Science, CAS Key Laboratory of Colloid, Interface and Chemical Thermodynamics, Institute of Chemistry, Chinese Academy of Sciences, No. 2 Zhongguancun Beiyijie, Beijing 100190, P. R. China

## S Supporting Information

**ABSTRACT:** In this paper, we report that cube-like Ag/AgCl nanostructures could be facily fabricated in a one-pot manner through a direct-precipitation protocol under ambient conditions, wherein no additional issues such as external energy (e.g., high temperature or high pressure), surfactants, or reducing agents are required. In terms of using sodium chloride (NaCl) as chlorine source and silver acetate ( $\text{CH}_3\text{COOAg}$ ) as silver source, it is disclosed that simply by adding an aqueous solution of NaCl into an aqueous solution of  $\text{CH}_3\text{COOAg}$ , Ag/AgCl nanostructures with a cube-like geometry, could be successfully formulated. We show that thus-formulated cube-like Ag/AgCl nanospecies could be used as high-performance yet durable visible-light-driven or sunlight-driven plasmonic photocatalysts for the photodegradation of methyl orange (MO) and 4-chlorophenol (4-CP) pollutants. Compared with the commercially available  $\text{P25-TiO}_2$ , and the Ag/AgCl nanospheres previously fabricated via a surfactant-assisted method, our current cube-like Ag/AgCl nanostructures could exhibit much higher photocatalytic performance. Our template free protocol might open up new and varied opportunities for an easy synthesis of cube-like Ag/AgCl-based high-performance sunlight-driven plasmonic photocatalysts for organic pollutant elimination.

**KEYWORDS:** silver/silver chloride, direct-precipitation, cube-like nanostructure, plasmonic photocatalyst, visible-light or sunlight, photodegradation



## 1. INTRODUCTION

As the industrialization and globalization proceed, few societies could be left untouched by environmental problems caused by organic pollutants.<sup>1–5</sup> To solve this significant issue, researchers have developed numerous semiconductor-based photocatalysts, traditionally exemplified by  $\text{TiO}_2$ -involved species, to fulfill the photodegradation of the organic pollutants.<sup>1–10</sup> However, because of its large band gap of ca. 3.2 eV, this kind of conventional photocatalyst is mainly catalytically active under UV light irradiation, which merely accounts for ca. 5% of solar energy.<sup>9–11</sup> Considering energy saving and utilization, sunlight or visible-light (which accounts for ca. 45% of solar energy), is the most promising energy source for the operation of the photocatalysts, due to their abundance, clean, economic and safe.<sup>9–11</sup> To a great extent, an efficient utilization of solar energy could mitigate our dependence on the fossil fuel, alleviate our energy consumption, and thus could reduce the  $\text{CO}_2$  emission.<sup>11,12</sup> It accordingly is a subject of general concern and paramount importance to develop sunlight-driven or visible-light-energized yet highly efficient and recyclable photocatalysts for the photodegradation of organic pollutants.<sup>9–11</sup>

Recently, the use of metallic nanostructures featured with evident surface plasmon resonance (SPR) absorptions in the

visible region, has been recognized to be an emerging alternative for the realization of an efficient conversion of solar energy to chemical energy for catalytic applications,<sup>12–22</sup> especially for the photodegradation of organic pollutants.<sup>12–30</sup>

Among diverse visible-light-driven plasmonic photocatalysts, cubically geometrized silver/silver chloride (Ag/AgCl)-based nanomaterials have gained particular attention.<sup>31–36</sup> This is owing to their outstanding catalytic performance, which is a result of the existence of fertile catalytically active sites, such as corners, edges, steps, etc.<sup>31,37–40</sup> Practically, to manufacture cube-like Ag/AgCl nanoarchitectures, template-directed protocols in terms of surfactant or ionic liquid-assisted assembly methods are generally employed.<sup>31–35</sup> In these cases, great efforts have to be applied to wash the abundant surfactants or ionic liquid, and sometimes an additional reducing step with regard to chemical reduction,<sup>33</sup> thermal<sup>34</sup> or light-induced<sup>35</sup> reduction has been used to generate metallic Ag species in the produced hybrids. In some other cases, cube-like AgCl precursors have to be presynthesized via a hydrothermal process, after which a light-induced formation of metallic Ag

**Received:** September 24, 2012

**Accepted:** November 8, 2012

**Published:** November 8, 2012

species has to be additionally involved.<sup>36</sup> Consequently, the launch of an original template free yet facile and efficient route for a one-pot and rapid synthesis of cube-like Ag/AgCl-based plasmonic photocatalysts remains a great challenge.

As a part of our sustained efforts in this topic,<sup>18,19,29–31</sup> we report herein our new efforts to manufacture cube-like plasmonic Ag/AgCl nanospecies via a facile direct-precipitation method under ambient conditions, wherein no templates such as surfactants or ionic liquid, and no other additional issues such as external energy (namely, high temperature, or high pressure) and reducing agents are required. It is demonstrated that simply by injecting an aqueous solution of sodium chloride (NaCl) dropwise into an aqueous solution silver acetate (CH<sub>3</sub>COOAg), cube-like Ag/AgCl nanospecies could be rapidly and facilely produced in a one-pot manner, wherein CH<sub>3</sub>COOAg and NaCl serve as the source of silver and chlorine, respectively. Our experimental results show that thus-synthesized cube-like Ag/AgCl nanoarchitectures could be employed as highly efficient yet stable plasmonic photocatalysts for the photodegradation of methyl orange (MO) and 4-chlorophenol (4-CP) pollutants under visible-light and sunlight irradiations. In contrast to the commercially available P25–TiO<sub>2</sub>, and the spherelike Ag/AgCl nanostructures previously synthesized via a surfactant-assisted method,<sup>29</sup> our present cube-like Ag/AgCl nanospecies display even higher photocatalytic performance.

The significance and advantage of our new protocol are two-fold. First, our template free strategy might be the first report that cube-like plasmonic Ag/AgCl nanomaterials could be facilely and more eco-friendly synthesized via a one-pot direct-precipitation method. No surfactants or ionic liquids, and no external energy (for examples, high temperature or high pressure), or reducing agents are essentially required during the synthesis procedure. These intrinsic merits, to a great extent, simplify the fabrication process to an extremely easy one. Second, our template-free method is easily expanded to a large-scale synthesis, which is a significant issue both in scientific and technological aspects. Our investigation might open up new and varied opportunities for the achievement of Ag/AgCl-based high-performance visible-light or sunlight-energized plasmonic photocatalysts for the photodegradation organic pollutants, which is a topic of paramount importance and general concern.

## 2. MATERIALS AND METHODS

**2.1. Materials.** Silver acetate (CH<sub>3</sub>COOAg, Alfa Aesar, >99%), sodium chloride (NaCl, >99.5%, Beijing Chemical Works, A.R.), methyl orange (MO, Alfa Aesar, >98%), and 4-chlorophenol (4-CP, Alfa Aesar, 99%) were used as received without additional purification or treatment. P25–TiO<sub>2</sub> (ca. 80% anatase and 20% rutile) nanospecies were purchased from Degussa and used as the reference photocatalysts for comparison.

**2.2. Synthesis of Cube-like Ag/AgCl Nanostructures via a Direct-Precipitation Method.** In a typical process, a 500  $\mu$ L aqueous solution of NaCl (0.2 M) was dropwise injected into a 10 mL aqueous solution of CH<sub>3</sub>COOAg (0.01 M) at room temperature under vigorous magnetic stirring within about 5 min. After the injection, the stirring was continuously maintained for another 20 min. The resultant dispersion was treated by centrifugation (10 000 rpm, 10 min) and the produced purplish red solids were collected and washed thoroughly with ultrapure Milli-Q water by repeating centrifugations. On the other hand, in order to achieve a

large scale synthesis, our cube-like Ag/AgCl nanostructures could also be facilely fabricated by using a 2.5 M aqueous solution of NaCl (4 mL) and a 0.1 M aqueous solution of CH<sub>3</sub>COOAg (100 mL). In this case, ca. 1.4 g of cube-like Ag/AgCl nanomaterials could be produced in one batch. Note that our Ag/AgCl nanostructures were fabricated in our laboratory under ambient conditions without special protections on sunny day or cloudy day with or without curtains, and the stock of the formulated nanostructures was also performed under the similar conditions. Under these ambient conditions, we measured the intensity of the ambient light during our nanofabrication, wherein the results showed that the intensity of the ambient light was about 0.05–0.75 mW cm<sup>-2</sup>. In practice, we found that approximately similar results could be obtained from the samples formulated under different intensity of the ambient light (0.05–0.75 mW cm<sup>-2</sup>). On the other hand, to verify that the generation of the metallic Ag<sup>0</sup> species in our samples was induced by the ambient light, similar synthesis works were also carried out in a strictly darkened room, wherein there was only a weak infrared lamp on the wall.

**2.3. Synthesis of Spherical Ag/AgCl Nanostructures via a Surfactant-Assisted Assembly Method.** The synthesis of the spherical Ag/AgCl nanospecies with a diameter of ca. 500 nm (see Figure S1 in the Supporting Information), whose dimension is similar as that of the cubic Ag/AgCl nanostructures synthesized in this present work, was carried out by means of a surfactant-assisted assembly method.<sup>29</sup> The calculated surface mole ratio estimated by means of the XPS spectra analysis between Ag<sup>0</sup> and Ag<sup>+</sup> was ca. 1:16.<sup>29</sup> These features were similar as those of the present cube-like Ag/AgCl nanostructures. The more detailed experimental operations were performed according to the methods described elsewhere.<sup>29</sup>

**2.4. Photocatalytic Performances.** For the photocatalytic experiments, photocatalysts typically involving 11 mg Ag/AgCl nanospecies were dispersed in a 12 mL aqueous solution of methyl orange (MO, 30 mg L<sup>-1</sup>) or 10 mL aqueous solution of 4-chlorophenol (4-CP, 16 mg L<sup>-1</sup>), wherein a quartz cuvette was used as the reactor. A 500 W xenon arc lamp installed in a laboratory lamp housing system (CHF–XM35–500 W, Beijing Trusttech Co. Ltd., China) was employed as the light source. The light passed through a 10 cm water filter and a UV cutoff filter (>400 nm) before entering the reactor. The reaction system was kept for 30 min in a dark room to achieve an equilibrium adsorption state before visible-light irradiation. Aliquot of the dispersion (0.5 mL) was taken out from the reaction system for the real-time sampling.

When the ambient sunlight was used as the energy source, photocatalysts typically involving ca. 11 mg Ag/AgCl nanostructures was dispersed in a 4 mL aqueous solution of MO pollutant (40 mg L<sup>-1</sup>) or 4 mL aqueous solution of 4-CP (40 mg L<sup>-1</sup>), wherein a quartz cuvette was used as the reactor. The system was kept for 30 min in dark to achieve an equilibrium adsorption state, after which the photodegradation experiments under ambient sunlight irradiation were carried out. Typically, the photocatalytic experiments were operated at the same time and the same place with the same sunlight intensity (ca. 50 mW cm<sup>-2</sup>) to make the data reasonably comparable. Aliquots of the dispersion (0.3 mL) were taken out from the reaction systems for the real-time sampling.

The progress of the photodegradation of MO and 4-CP pollutants over our photocatalysts was investigated by measuring the real-time UV–vis absorption of MO and 4-CP

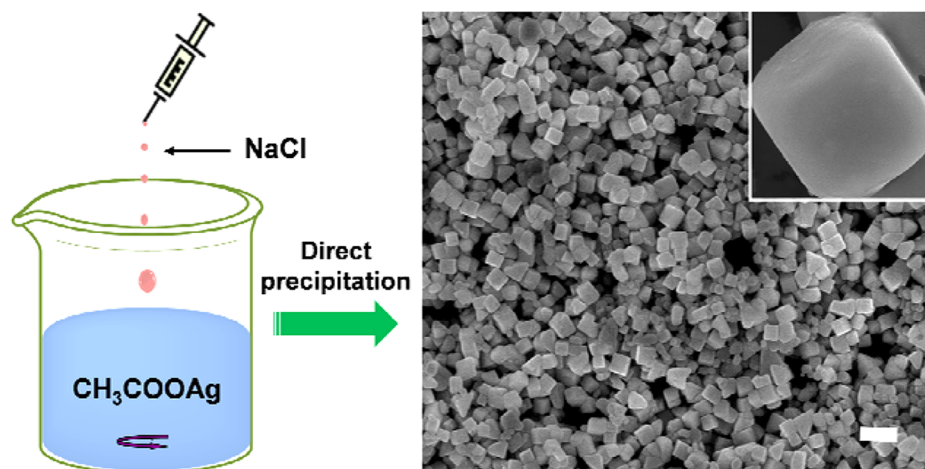


**Figure 1.** Schematic illustration for the synthesis of cube-like Ag/AgCl nanostructures via a simple one-pot direct-precipitation method, and the SEM image of the products. The scale bar indicates 1  $\mu\text{m}$ . The inset in the right panel is the enlarged SEM image of a cube-like nanostructure.

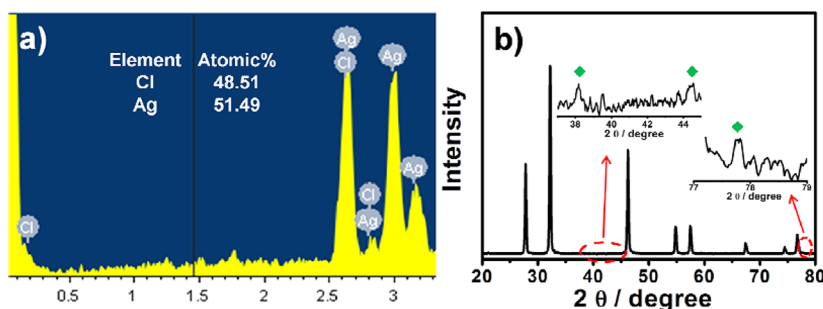


**Figure 2.** (a) EDX and (b) XRD spectra of the cube-like Ag/AgCl nanostructures. The semiquantitative elemental analysis result is listed in the EDX panel. The diffraction peaks ascribing to the metallic  $\text{Ag}^0$  are marked with  $\blacklozenge$  in the inset of the XRD spectrum.

at 463 and 280 nm, respectively. For the evaluation of the photocatalytic activities,  $C$  is the concentration of MO or 4-CP at a real-time  $t$ , and  $C_0$  is that in the MO or 4-CP solution immediately before it was kept in the dark. For comparison, we also investigated the photocatalytic performance of the commercially available P25- $\text{TiO}_2$ , and the spherical Ag/AgCl nanospecies previously synthesized via a surfactant-assisted method.<sup>29</sup> In these cases, ca. 11 mg of these referenced photocatalysts were employed to make the obtained data reasonably comparable.

**2.5. Apparatus and Measurements.** The scanning electron microscopy (SEM) measurements were carried out by using a Hitachi S-4800 system, wherein an accelerating voltage of 10 kV was employed. The energy dispersive X-ray spectroscopy (EDX) was measured with a Horiba EMAX X-ray energy dispersive spectroscopy that was attached to the Hitachi S-4800 system. In this case, an accelerating voltage of 15 kV was employed. X-ray photoelectron spectroscopy (XPS) was performed on an ESCALab220i-XL electron spectrometer from VG Scientific using 300W Al  $K\alpha$  radiation. The binding energies were referenced to the C1s line at 284.8 eV from adventitious carbon. X-ray diffraction (XRD) measurements were performed on a PANalytical X'Pert PRO instrument with Cu  $K\alpha$  radiation. The transmission electron microscopy (TEM) of the cube-like nanostructures was investigated with a JEOL JEM-2011, which was operated with an accelerating voltage of 200 kV. UV-vis diffuse reflectance spectra of the samples were obtained on an UV-vis spectrophotometer (Hitachi U-3010) using  $\text{BaSO}_4$  as the reference. The photodegradation of the MO

and 4-CP pollutants was monitored by using a JASCO UV-550 spectrophotometer. The specific surface areas of our plasmonic photocatalysts were measured by means of nitrogen gas adsorption at  $-196^\circ\text{C}$  using a TriStar II 3020 (Micromeritics, USA) after the samples were degassed in vacuum at  $120^\circ\text{C}$  overnight, and the specific surface areas were estimated in terms of the Brunauer-Emmett-Teller (BET) method. All the measurements and experiments were carried out at ambient temperature except where noted.

### 3. RESULTS AND DISCUSSION

**3.1. Synthesis and Characterization of Cube-like Ag/AgCl Nanostructures.** Experimentally, as schematically illustrated in Figure 1, our cube-like Ag/AgCl nanostructures could be easily manufactured by means of adding an aqueous solution of NaCl (500  $\mu\text{L}$ , 0.2 M, average dropping speed ca. 100  $\mu\text{L min}^{-1}$ ) dropwise into an aqueous solution of  $\text{CH}_3\text{COOAg}$  (10 mL, 0.01 M). During this synthesis procedure,  $\text{CH}_3\text{COOAg}$  works as silver source, whereas NaCl serves as chlorine source. As shown in the right panel of Figure 1, the typical SEM image of thus-synthesized products indicates that cube-like nanostructured species with a size of ca. 500 nm could be produced. Experimentally, we also expanded this protocol to a large scale synthesis. In this case, an aqueous solution of NaCl (4 mL, 2.5 M, average dropping speed ca. 0.8 mL  $\text{min}^{-1}$ ) was injected dropwise into an aqueous solution of  $\text{CH}_3\text{COOAg}$  (100 mL, 0.1 M), and ca. 1.4 g of products could be produced in one batch. As indicated in Figure S2 in the Supporting Information, a similar result is obtained. This result



suggests that our new method could be handily expanded to large-scale synthesis.

To validate the generation of Ag/AgCl nanospecies, the components of the thus-manufactured cube-like nanostructures are investigated by means of energy dispersive X-ray spectroscopy (EDX) analysis. As shown in Figure 2a, Ag and Cl elements could be evidently detected, wherein the semi-quantitative analysis shows that the atomic ratio between Ag and Cl elements is approximately 1.06:1. This data is higher than the theoretic stoichiometric atomic ratio between Ag and Cl species in AgCl, which should be 1:1. This experimental fact basically suggests an ambient light induced generation of metallic Ag<sup>0</sup> species in the cube-like nanostructures, which could result in the formation of Ag/AgCl nanospecies.<sup>29,31</sup> The X-ray diffraction (XRD) patterns of our nanostructures was also investigated to identify the formation of Ag/AgCl nanospecies. As shown in Figure 2b, distinct diffraction peaks (2 $\theta$ ) at 27.7° (111), 32.1° (200), 46.2° (220), 54.7° (311), 57.4° (222), 67.4° (400), 74.4° (331), and 76.6° (420) could be unambiguously detected. These diffraction peaks are attributed to the typical cubic phase of AgCl (JCPDS file: 31-1238), suggesting the formation of the AgCl species in our synthesized nanostructures.<sup>23,24</sup> At the same time, as shown in the inset of Figure 2b, a careful observation of the XRD pattern indicates that diffraction peaks at 38.2° (111), 44.6° (200) and 77.9° (311), could also be detected from the same XRD spectrum. These diffraction peaks are ascribed to the typical cubic phase of metallic Ag (JCPDS file: 65-2871), solidly verifying the existence of Ag<sup>0</sup> species in our cube-like nanostructures.<sup>23,24</sup> As a result, together with the experimental results deduced from the EDX analyses, this XRD investigation solidly verifies the formation of the cube-like Ag/AgCl nanostructures.

To further confirm the existence of metallic Ag<sup>0</sup> species in the produced cube-like nanostructures, we carried out X-ray photoelectron spectroscopy (XPS) investigations, as shown in Figure 3. On one hand, the Cl species display a binding energy

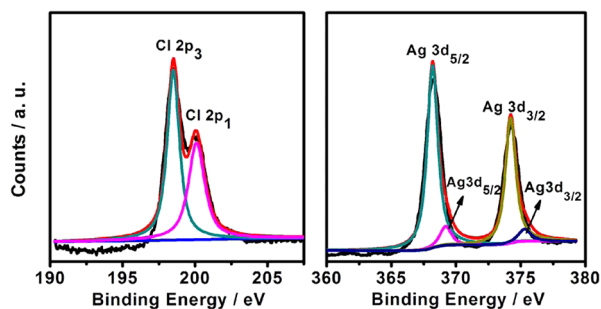


**Figure 3.** Typical XPS spectra of (a) Cl 2p and (b) Ag 3d of the cube-like Ag/AgCl nanostructures.

of Cl 2p<sub>3</sub> and Cl 2p<sub>1</sub> at about 198.0 and 199.5 eV, respectively (Figure 3a).<sup>24,30–32</sup> On the other hand, for the XPS spectra of the Ag species shown in Figure 3b, two band at ca. 368.2 and 374.2 eV, ascribing to Ag 3d<sub>5/2</sub> and Ag 3d<sub>3/2</sub> binding energies, respectively, are observed. These bands could be further deconvoluted into two peaks, respectively, at 367.5, 368.4 eV and 373.5, 374.4 eV. Those at 367.5 and 373.5 eV could be attributed to the Ag<sup>+</sup> of AgCl, while those at 368.4 and 374.4 eV could be ascribed to the metallic Ag<sup>0</sup>.<sup>23,24,29–31</sup> The semi-quantitatively calculated surface mole ratio between Ag<sup>0</sup> and Ag<sup>+</sup> is approximately 1:16. These results further indicate

the existence of Ag<sup>0</sup> species in the obtained cube-like nanospecies.

As it is widely verified, for visible-light or sunlight-energized photocatalysts, it is essentially required that they could display distinct absorptions in visible region so as to achieve an efficient energy supply and a high catalytic performance. Figure 4

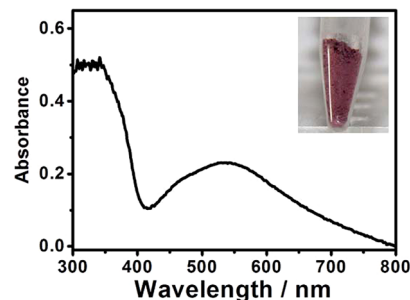


**Figure 4.** Typical UV-visible diffuse reflectance spectrum of the cube-like Ag/AgCl nanostructures. Inset: the photograph of thus-obtained sample.

illustrates the UV-visible diffuse reflectance spectrum and a photograph of the as-prepared cube-like Ag/AgCl nanostructures. It can be seen that the sample displays a purplish red color, from which broad and strong absorptions in visible region could be evidently detected. Generally, the bare AgCl species could only display negligible absorption in the visible region.<sup>23,34</sup> Accordingly, accompanied by the experimental results derived from the above-described EDX, XRD and XPS investigations, the present result solidly indicating the existence of Ag<sup>0</sup> species in our cube-like nanostructures, which could arouse distinct SPR absorptions in the visible region.<sup>23,24,31</sup> As a matter of fact, we have also attempted to disclose the internal structures of our cube-like nanostructures by means of TEM. It failed, however, because it was found that our nanostructures suffered a fast decomposition under the high-energy electron beam of the TEM, as shown in Figure S3 in the Supporting Information. A similar phenomenon was reported previously.<sup>27,31</sup> Nevertheless, the aforementioned experimental facts strongly confirm the existence of the metallic Ag<sup>0</sup> species in our nanostructures. This intrinsic feature might make our cube-like Ag/AgCl nanospecies catalytically active under visible-light or sunlight irradiation.<sup>23</sup>

To verify that the generation of the metallic Ag<sup>0</sup> species is induced by the ambient light during our synthesis procedure, we have additionally carried out similar synthesis work in a strictly darkened room, wherein there is only a weak infrared lamp on the wall.<sup>29</sup> In these cases, as shown in the inset of Figure S4 in the Supporting Information, instead of a purplish red color, thus-obtained products manifest themselves as white powders. More importantly, they could display only negligible SPR absorptions in the visible region (see Figure S4 in the Supporting Information), suggesting the generation of the Ag<sup>0</sup> species could be nearly forbidden under this synthesis circumstance. This deduction could be further confirmed by the EDX spectrum of the as-formulated samples, wherein the atomic ratio between Ag and Cl elements is semi-quantitatively estimated to be ca. 1:1, very close to the theoretic stoichiometric atomic ratio between Ag and Cl species in AgCl, as shown in Figure S5 in the Supporting Information. Compared with the results observed from those samples produced under the ambient conditions, these experimental

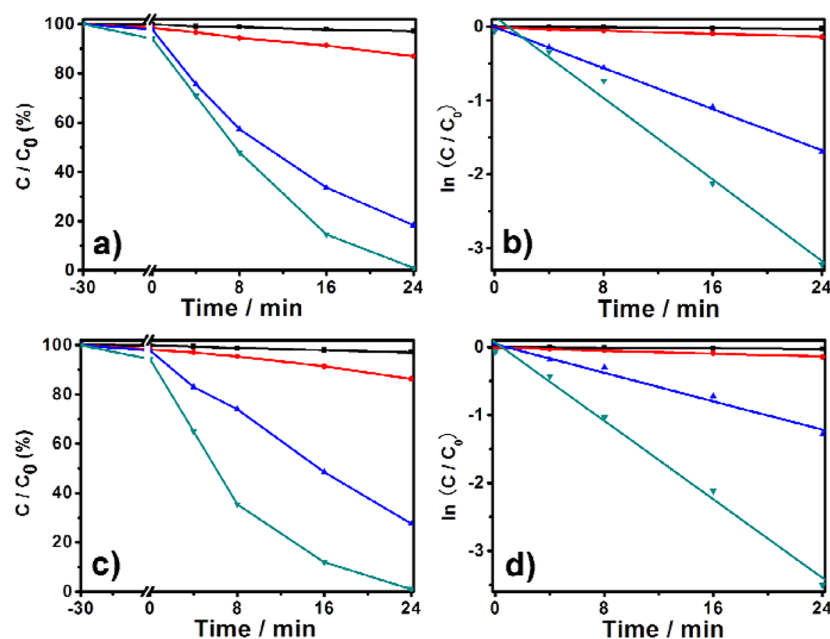


**Figure 5.** (a, c) Photocatalytic performances and (b, d) kinetic linear simulation curves of the investigated photocatalysts (■, a blank experiment, where no catalyst is used; ●, commercially available P25–TiO<sub>2</sub>; ▲, spherical Ag/AgCl nanospecies; ▼, cube-like Ag/AgCl nanostructures) for the photodegradation of (a, b) MO and (c, d) 4-CP pollutants under visible-light irradiation.

facts suggest that the generation of Ag<sup>0</sup> species in our Ag/AgCl nanostructures is substantially induced by the ambient light.

**3.2. Photocatalytic Performance of the Cube-like Ag/AgCl Nanostructures for the Photodegradation of Organic Pollutants under Visible-Light and Sunlight Irradiation.** The photocatalytic performance of our cube-like Ag/AgCl nanostructures was investigated in terms of the photodegradation of MO (Figure 5a and 5b) and 4-CP (Figure 5c and 5d) pollutants under visible-light irradiation. Practically, the photocatalytic process was monitored by means of measuring the real-time UV–vis absorption of MO and 4-CP pollutants at a wavelength of 463 and 280 nm, respectively. Prior to the light irradiation, a dark adsorption experiment was performed to achieve an equilibrium adsorption state. As shown in Figure 5, when no catalysts are involved in the reaction system, negligible photodegradation of MO and 4-CP pollutants could be achieved under visible-light irradiation. This suggests that the self-photo-sensitized decomposition of these organic pollutants under our experimental conditions could basically be ignored. On the other hand, when the commercially available P25–TiO<sub>2</sub> is used as the photocatalyst, only a slight photodegradation of these organic molecules could be observed within 24 min, indicating the less photocatalytic performance of the commercially available P25–TiO<sub>2</sub> under our experimental conditions. In contrast, when our present cube-like Ag/AgCl nanostructures are employed as the photocatalysts, nearly 100% MO and 4-CP molecules are photodecomposed under the similar experimental conditions. For comparison, 81.6% and 72.5% MO and 4-CP molecules are photodecomposed, respectively, when the spherical Ag/AgCl nanostructures, which were previously synthesized via a surfactant-assisted method,<sup>29</sup> are used as the photocatalysts. Note that the diameter of these spherical nanostructures was ca. 500 nm (see Figure S1 in the Supporting Information), and the semiquantitatively calculated surface mole ratio between Ag<sup>0</sup> and Ag<sup>+</sup> was also ca. 1:16. These data are similar to those of our present cube-like Ag/AgCl nanostructures.

As plotted in Figure 5b and 5d, there is a nice linear correlation between  $\ln(C/C_0)$  and the reaction time ( $t$ ). This experimental fact indicates that both the photodecomposition reaction of MO and 4-CP molecules photocatalyzed by our catalysts follows the first-order kinetics:<sup>19,30</sup>

$$-\frac{dC}{dt} = kC$$

wherein  $C$  stands for the real-time concentration of the MO or 4-CP molecules,  $t$  represents the reaction time, and  $k$  stands for the rate constant. The rate constant of the photocatalytic degradation of MO and 4-CP over our cube-like Ag/AgCl nanostructures is determined to be 0.134 min<sup>-1</sup> and 0.144 min<sup>-1</sup>, respectively, which are distinctly higher than that of the previously synthesized spherical Ag/AgCl nanospecies (0.069 min<sup>-1</sup> for MO, and 0.052 min<sup>-1</sup> for 4-CP). These experimental facts suggest that compared with their spherical counterpart of similar dimension and component,<sup>29</sup> our present cube-like Ag/AgCl nanoarchitectures are high-performance plasmonic photocatalysts for the elimination of organic pollutants under visible-light illumination.

As it is known, besides the excellent catalytic activity, the recyclability of the catalysts is another principle substantially required by high-quality catalytic species. The durability of our cube-like Ag/AgCl-based plasmonic photocatalysts was also evaluated in terms of performing the MO and 4-CP bleaching reactions repeatedly several times. As shown in Figure 6, the catalytic performances of our catalysts in terms of the photodegradation MO and 4-CP molecules display only trivial decrease under visible-light irradiation after the performances are operated five times continuously and consecutively. Moreover, as shown in Figure S6 in the Supporting Information, the morphology of our cube-like Ag/AgCl nanostructures displays only slight changes after the bleaching reactions. These experimental facts suggest that our cube-like Ag/AgCl nanomaterials could be employed as stable plasmonic

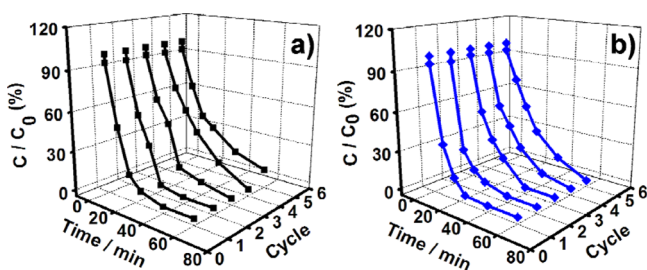


**Figure 6.** Five consecutive cycling degradation curves of (a) MO and (b) 4-CP over our cube-like Ag/AgCl nanostructures under visible light irradiation.

photocatalysts for the bleaching of organic pollutants under visible light irradiation.

In practice, from the point of view of energy saving and utilization, sunlight, which is the most economical and renewable energy source, should be the most attractive candidate to supply energy for the performance of the photocatalysts.<sup>9–11</sup> The catalytic performances of the commercially available P25–TiO<sub>2</sub>, the spherical Ag/AgCl nanostructures, and our present cube-like Ag/AgCl nanostructures, are also evaluated in terms of the photodegradation of MO and 4-CP pollutants under direct sunlight irradiation. Note that all of these experiments were performed at the same time and the same place with the same sunlight intensity to make the data reasonably comparable. As shown in Figure 7, when the commercially available P25–TiO<sub>2</sub> species is used as the photocatalysts, only a slight decomposition of these organic pollutants could be achieved within 15 min, indicating the less photocatalytic performance of the commercially available P25–TiO<sub>2</sub> species. In contrast, when our present cube-like Ag/AgCl nanostructures are employed as the photocatalysts, nearly 100% MO and 80% 4-CP molecules could be decomposed under the similar experimental conditions. For comparison, 62.3% and

55% MO and 4-CP molecules are photodecomposed, respectively, when the spherical Ag/AgCl nanostructures, which were previously synthesized via a surfactant-assisted method,<sup>29</sup> are used as the photocatalysts. At the same time, it could be seen that the rate constant of the photodegradation of MO and 4-CP over our cube-like Ag/AgCl nanostructures are determined to be 0.257 and 0.095 min<sup>-1</sup>, respectively. These values are evidently higher than those of the corresponding spherical Ag/AgCl (0.06 and 0.051 min<sup>-1</sup>) nanospecies. This tendency is similar to that obtained when the catalytic systems are energized by visible-light irradiation (Figure 5). These experimental facts indicate the bright future of our cube-like Ag/AgCl as photocatalysts for future potential applications.

As shown in Figures 5a, 5c, 7a, and 7c, our cube-like Ag/AgCl nanostructures have a higher adsorptive ability for pollutant molecules than the spherical Ag/AgCl nanospecies. This might be ascribed to the higher specific surface area of the polyhedron-shaped nanostructures than their spherical counterparts of similar size, which could partially contribute to their higher catalytic activities.<sup>31,37,38</sup> To confirm this proposal, the specific surface areas of our Ag/AgCl-based plasmonic photocatalysts were estimated by means of the BET method. The results show that the BET surface areas of our cube-like and spherical Ag/AgCl nanostructures are estimated to be ca. 0.56 and 0.34 m<sup>2</sup> g<sup>-1</sup>, respectively. These data are very close to those of the Ag/AgX-based (X = PO<sub>4</sub>, Br, and Cl) plasmonic photocatalysts reported by others.<sup>41</sup> At the same time, it can be seen that the BET surface area of our cube-like Ag/AgCl nanostructures is larger than that of their spherical counterparts. This is in accordance with the experimental fact that the cube-like Ag/AgCl nanostructures have a higher adsorptive ability for pollutant molecules than the spherical Ag/AgCl nanospecies, verifying that the higher specific surface area of our cube-like Ag/AgCl nanostructures might contribute partially to their higher catalytic activities. Moreover, as it is well-known that compared with the spherical nanospecies,

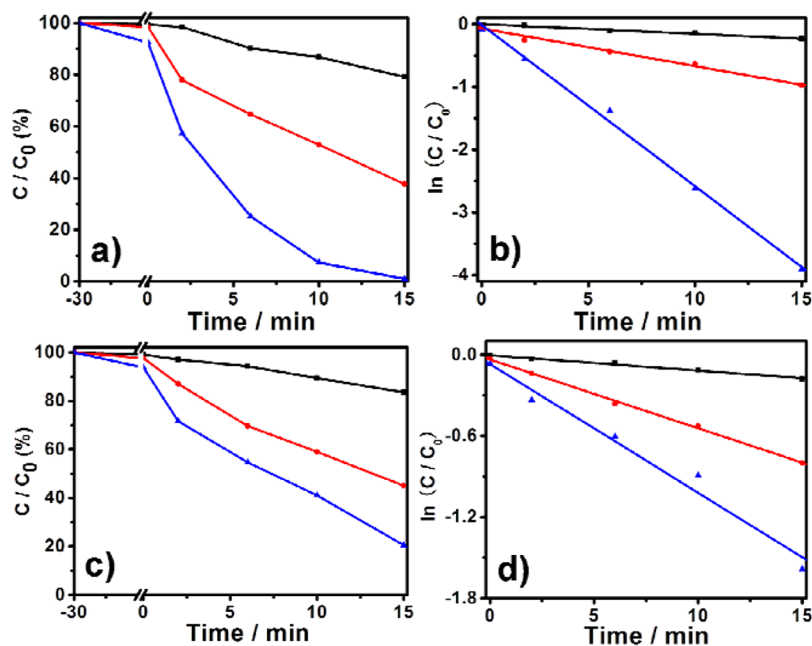


**Figure 7.** (a, c) Photocatalytic performances and (b, d) kinetic linear simulation curves of our photocatalysts (■, commercially available P25–TiO<sub>2</sub>; ●, spherical Ag/AgCl nanostructures; ▲, cube-like Ag/AgCl nanospecies) for the degradation of (a, b) MO and (c, d) 4-CP pollutants under direct sunlight irradiation.



there exist more fertile catalytically active sites (corners, edges, steps, etc.) and active facets in the cubic counterparts.<sup>37–40</sup> This factor might also contribute partially to the higher catalytic performance of our cube-like Ag/AgCl nanostructures.

#### 4. CONCLUSIONS

In conclusion, we herein report that cube-like Ag/AgCl nanostructures could be facilely synthesized via a facile template free one-pot direct-precipitation method on a large scale, wherein CH<sub>3</sub>COOAg works as Ag source and NaCl works as Cl source, respectively. The remarkable merit of our new synthesis protocol is that the synthesis of the cube-like Ag/AgCl nanomaterials can be achieved easily in a one-step manner under ambient conditions without any external energy (e.g., high temperature or high pressure), surfactants, ionic liquids, or reducing agents. Thus-obtained cube-like Ag/AgCl nanostructures could be used as high-performance yet durable visible-light-energized or sunlight-driven plasmonic photocatalysts for the photodegradation of organic pollutants. Compared with commercially available P25–TiO<sub>2</sub> species and the spherical Ag/AgCl nanostructures, our current cube-like Ag/AgCl nanostructures could exhibit much higher photocatalytic performances. Our new protocol might open up a new avenue for an easy synthesis of cube-like Ag/AgCl-based high-performance yet stable visible-light or sunlight driven plasmonic photocatalysts for organic pollutant elimination.

#### ■ ASSOCIATED CONTENT

##### Supporting Information

SEM images of the spherical Ag/AgCl nanostructures previously formulated *via* a surfactant-assisted method, of the cube-like Ag/AgCl nanostructures produced by a large scale synthesis, and of the cube-like Ag/AgCl nanospecies after the photocatalytic degradation of MO and 4-CP under visible-light irradiation, TEM image of the cube-like Ag/AgCl nanospecies, UV-visible diffuse reflectance spectrum, photograph and EDX spectrum of the AgCl species fabricated in a strictly darkened room. This information is available free of charge via the Internet at <http://pubs.acs.org/>.

#### ■ AUTHOR INFORMATION

##### Corresponding Author

\*E-mail: chenpl@iccas.ac.cn; liumh@iccas.ac.cn. Fax: (+) 86–10–62569564. Tel: (+) 86–10–82615803.

##### Notes

The authors declare no competing financial interest.

#### ■ ACKNOWLEDGMENTS

The authors acknowledge the financial support from National Natural Science Foundation of China (20873159, 21021003 and 91027042), the Ministry of Science and Technology of China (2011CB932301 and 2013CB834504), and the Chinese Academy of Sciences. The authors are grateful to Prof. Bao-Hang Han and Dr Li-Juan Mao from the National Center for Nanoscience and Technology for their great helps in the measurement and in-depth discussions of the BET surface areas of the nanostructures.

#### ■ REFERENCES

(1) Legrini, O.; Oliveros, E.; Braun, A. M. *Chem. Rev.* **1993**, *93*, 671–698.

- (2) Bhatkhande, D. S.; Pangarkar, V. G.; Beenackers, A. A. C. M. *J. Chem. Technol. Biotechnol.* **2002**, *77*, 102–116.
- (3) Hoffmann, M. R.; Martin, S. T.; Choi, W.; Bahnemann, D. W. *Chem. Rev.* **1995**, *95*, 69–96.
- (4) Mills, A.; Davies, R. H.; Worsley, D. *Chem. Soc. Rev.* **1993**, *22*, 417–425.
- (5) Zhang, D.; Li, G.; Yu, J. C. *J. Mater. Chem.* **2010**, *20*, 4529–4536.
- (6) Chen, X.; Mao, S. S. *Chem. Rev.* **2007**, *107*, 2891–2959.
- (7) Linsebigler, A. L.; Lu, G.; Yates, J. T. *Chem. Rev.* **1995**, *95*, 735–758.
- (8) Fujishima, A.; Rao, T. N.; Tryk, D. A. *J. Photochem. Photobiol. C: Photochem. Rev.* **2000**, *1*, 1–21.
- (9) Zhao, J.; Chen, C.; Ma, W. *Top. Catal.* **2005**, *35*, 269–278.
- (10) Chen, C.; Ma, W.; Zhao, J. *Chem. Soc. Rev.* **2010**, *39*, 4206–4219.
- (11) Kubacka, A.; Fernández-García, M.; Colón, G. *Chem. Rev.* **2011**, *112*, 1555–1614.
- (12) Chen, X.; Zheng, Z.; Ke, X.; Jaatinen, E.; Xie, T.; Wang, D.; Guo, C.; Zhao, J.; Zhu, H. *Green Chem.* **2010**, *12*, 414–419.
- (13) Awazu, K.; Fujimaki, M.; Rockstuhl, C.; Tominaga, J.; Murakami, H.; Ohki, Y.; Yoshida, N.; Watanabe, T. *J. Am. Chem. Soc.* **2008**, *130*, 1676–1680.
- (14) Christopher, P.; Xin, H.; Linic, S. *Nat. Chem.* **2011**, *3*, 467–472.
- (15) Liu, Z.; Hou, W.; Pavaskar, P.; Aykol, M.; Cronin, S. B. *Nano Lett.* **2011**, *11*, 1111–1116.
- (16) Chen, X.; Zhu, H.-Y.; Zhao, J.-C.; Zheng, Z.-F.; Gao, X.-P. *Angew. Chem., Int. Ed.* **2008**, *47*, 5353–5356.
- (17) Zhu, H.; Ke, X.; Yang, X.; Sarina, S.; Liu, H. *Angew. Chem., Int. Ed.* **2010**, *49*, 9657–9661.
- (18) Zhu, M.; Chen, P.; Liu, M. *Langmuir* **2012**, *28*, 3385–3390.
- (19) Zhu, M.; Chen, P.; Liu, M. *Chin. Sci. Bull.* **2012**, DOI: 10.1007/s11434-012-5367-9.
- (20) Wang, P.; Huang, B.; Dai, Y.; Whangbo, M.-H. *Phys. Chem. Chem. Phys.* **2012**, *14*, 9813–9825.
- (21) Zhou, X.; Liu, G.; Yu, J.; Fan, W. *J. Mater. Chem.* **2012**, *22*, 21337–21354.
- (22) Linic, S.; Christopher, P.; Ingram, D. B. *Nat. Mater.* **2011**, *10*, 911–921.
- (23) Wang, P.; Huang, B.; Qin, X.; Zhang, X.; Dai, Y.; Wei, J.; Whangbo, M.-H. *Angew. Chem., Int. Ed.* **2008**, *47*, 7931–7933.
- (24) Wang, P.; Huang, B.; Lou, Z.; Zhang, X.; Qin, X.; Dai, Y.; Zheng, Z.; Wang, X. *Chem.—Eur. J.* **2010**, *16*, 538–544.
- (25) Xu, H.; Li, H.; Xia, J.; Yin, S.; Luo, Z.; Liu, L.; Xu, L. *ACS Appl. Mater. Interfaces* **2010**, *3*, 22–29.
- (26) Yu, J.; Dai, G.; Huang, B. *J. Phys. Chem. C* **2009**, *113*, 16394–16401.
- (27) Jiang, J.; Zhang, L. *Chem.—Eur. J.* **2011**, *17*, 3710–3717.
- (28) Li, Y.; Ding, Y. *J. Phys. Chem. C* **2010**, *114*, 3175–3179.
- (29) Zhu, M.; Chen, P.; Liu, M. *ACS Nano* **2011**, *5*, 4529–4536.
- (30) Zhu, M.; Chen, P.; Liu, M. *J. Mater. Chem.* **2012**, *22*, 21487–21494.
- (31) Zhu, M.; Chen, P.; Liu, M. *J. Mater. Chem.* **2011**, *21*, 16413–16419.
- (32) Chen, D.; Yoo, S. H.; Huang, Q.; Ali, G.; Cho, S. O. *Chem.—Eur. J.* **2012**, *18*, 5192–5200.
- (33) An, C.; Wang, R.; Wang, S.; Zhang, X. *J. Mater. Chem.* **2011**, *21*, 11532–11536.
- (34) An, C.; Peng, S.; Sun, Y. *Adv. Mater.* **2010**, *22*, 2570–2574.
- (35) Lou, Z.; Huang, B.; Wang, P.; Wang, Z.; Qin, X.; Zhang, X.; Cheng, H.; Zheng, Z.; Dai, Y. *Dalton Trans.* **2011**, *40*, 4104–4110.
- (36) Han, L.; Wang, P.; Zhu, C.; Zhai, Y.; Dong, S. *Nanoscale* **2011**, *3*, 2931–2935.
- (37) Wang, D.; Xie, T.; Li, Y. *Nano Res.* **2009**, *2*, 30–46.
- (38) Chen, J.; Lim, B.; Lee, E. P.; Xia, Y. *Nano Today* **2009**, *4*, 81–95.
- (39) Semagina, N.; Kiwi-Minsker, L. *Catal. Rev.* **2009**, *51*, 147–217.
- (40) Li, Y.; Liu, Q.; Shen, W. *Dalton Trans.* **2011**, *40*, 5811–5826.
- (41) Liu, Y.; Fang, L.; Lu, H.; Li, Y.; Hu, C.; Yu, H. *Appl. Catal. B: Environ.* **2012**, *115–116*, 245–252.